Supplement of The Cryosphere, 20, 2773–2792, 2026
https://doi.org/10.5194/tc-20-2773-2026-supplement

The Cryosphere Open Access EGU

Supplement of

Assimilation of synthetic observations of radar backscatters at Ku-band improves SWE estimates

Nicolas R. Leroux et al.

Correspondence to: Nicolas R. Leroux (nicolas.leroux@ec.gc.ca)

S1 Additional figures

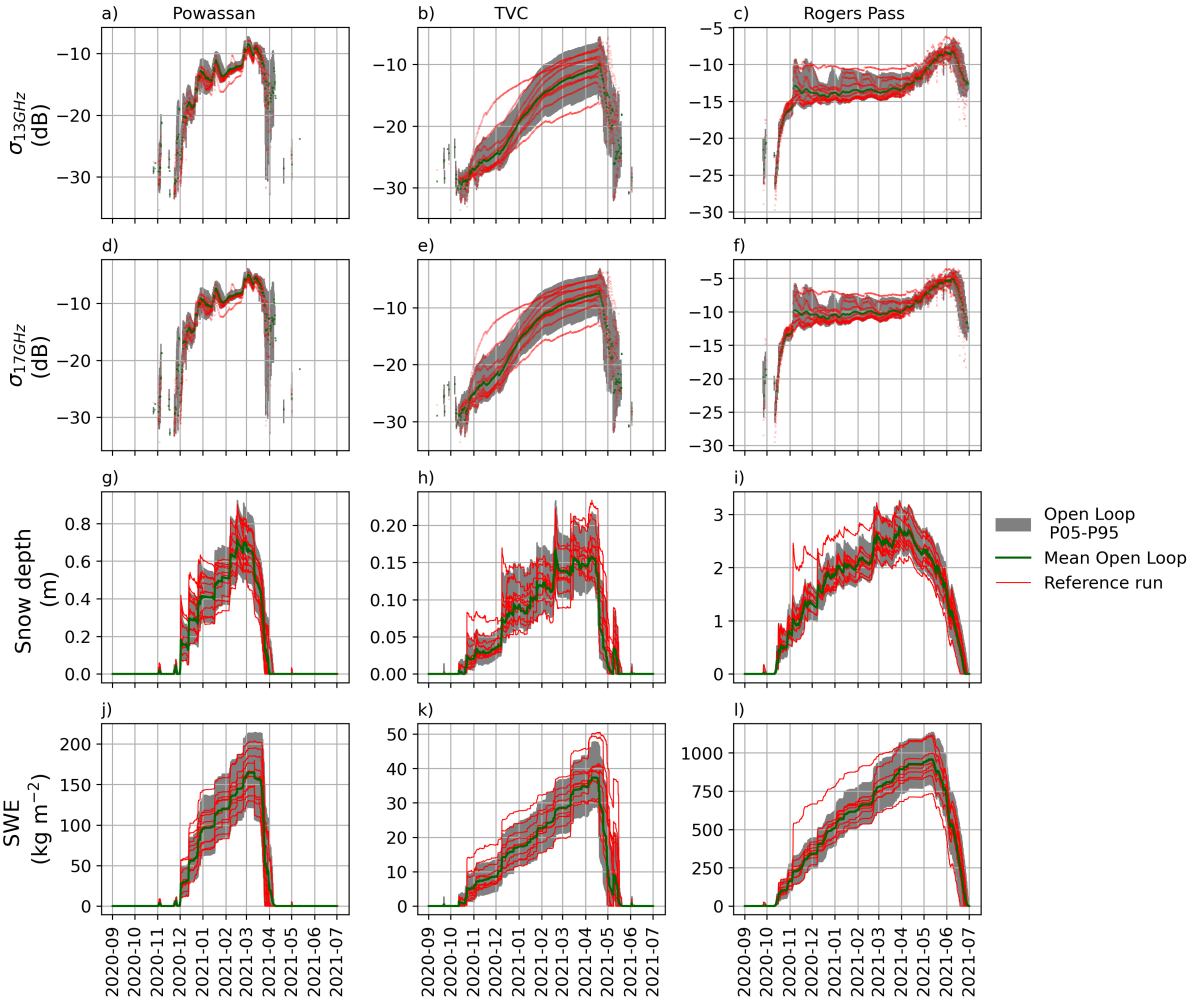

Figure S1. Spread of the open loop (OL) ensemble (between 5th and 95th percentiles) and the 10 reference runs at (a, d, g, j) Powassan, (b, e, h, k) TVC , and (c, f, i, l) Rogers Pass for (a-c) the backscatter at 13.5 GHz, (d-f) the backscatter at 17.25 GHz, (g-i) for snow height , and (j-l) SWE for the winter 2020-2021.

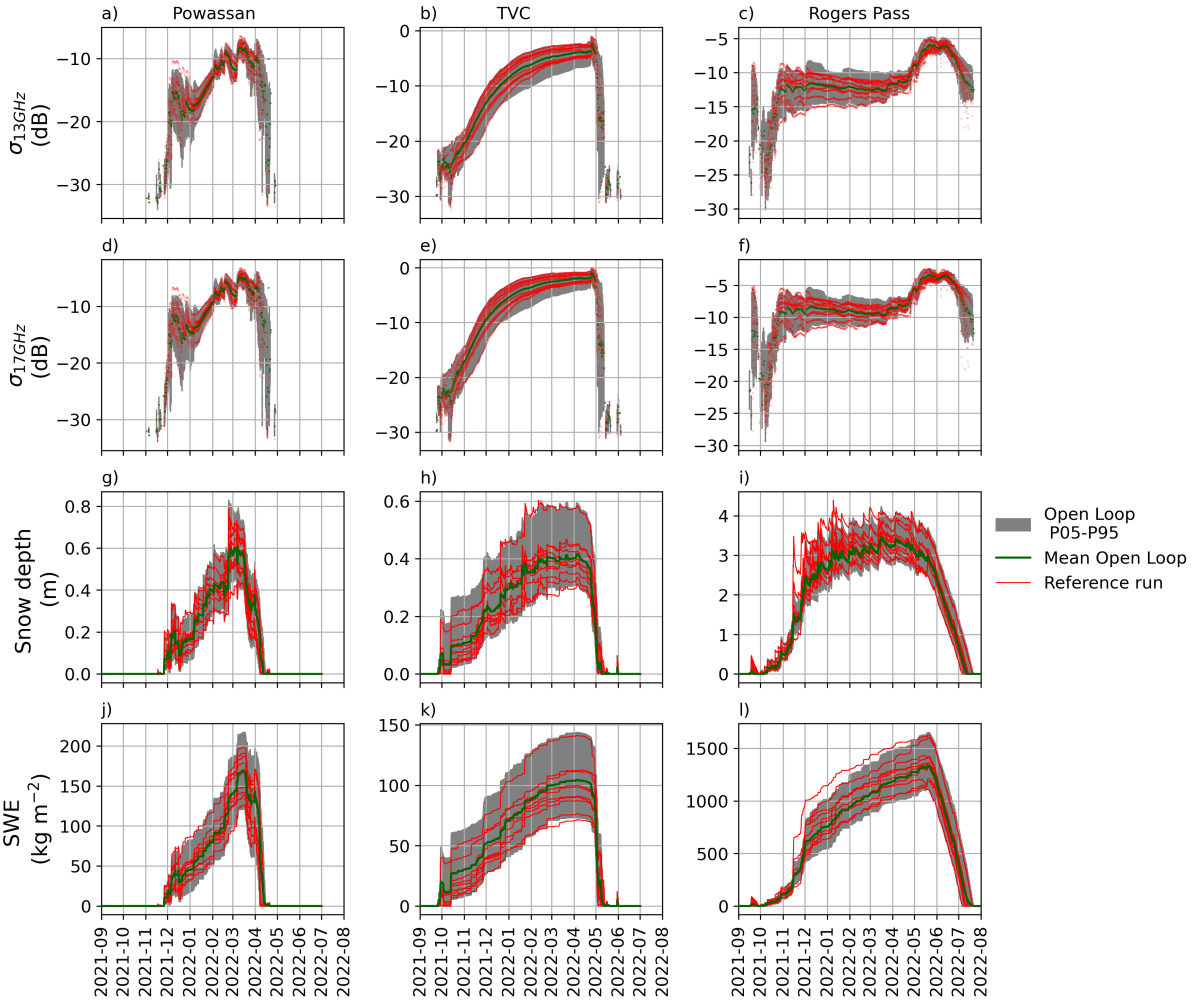

Figure S2. Spread of the open loop (OL) ensemble (between 5th and 95th percentiles) and the 10 reference runs at (a, d, g, j) Powassan, (b, e, h, k) TVC , and (c, f, i, l) Rogers Pass for (a-c) the backscatter at 13.5 GHz, (d-f) the backscatter at 17.25 GHz, (g-i) for snow height , and (j-l) SWE for the winter 2021-2022.

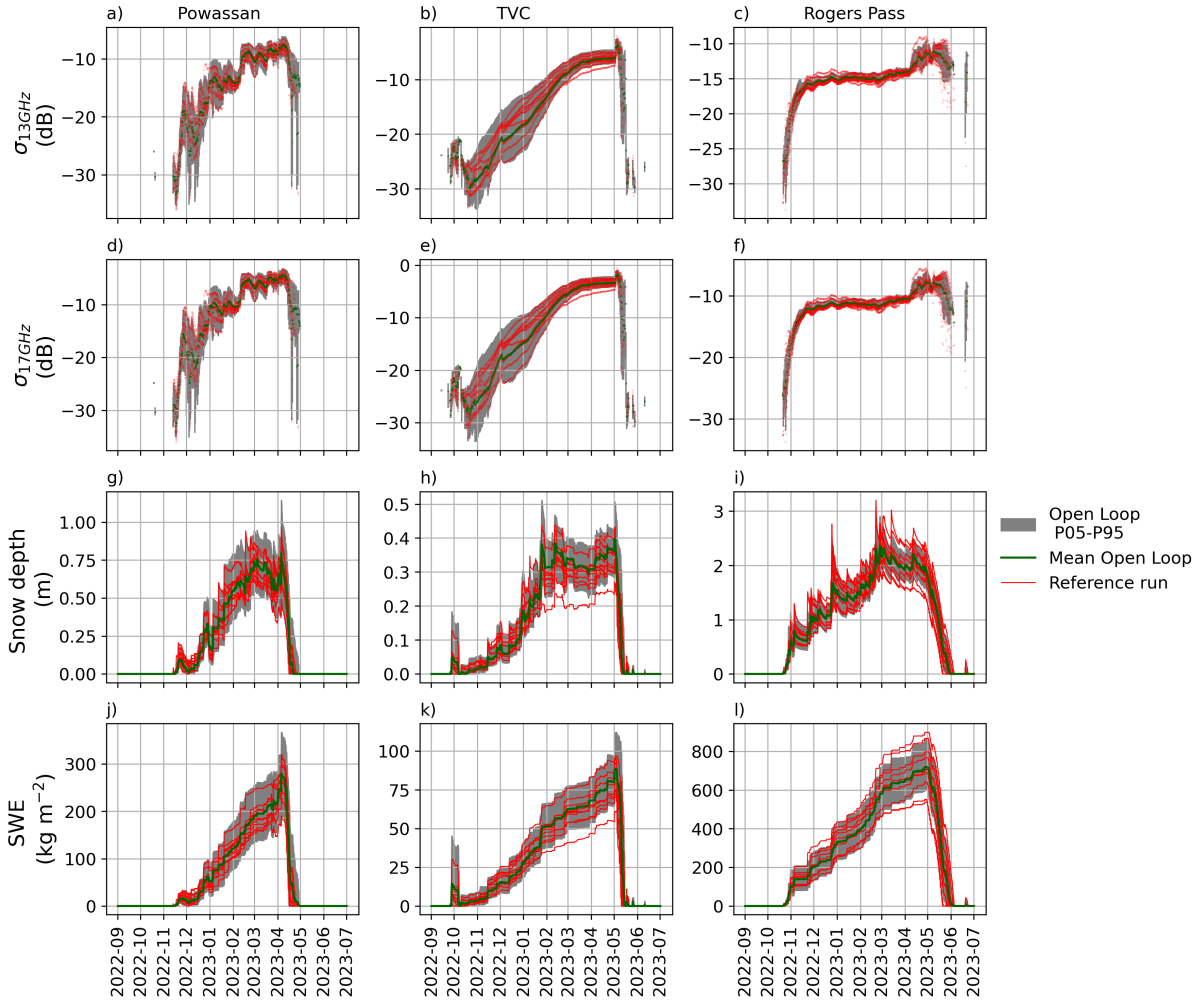

Figure S3. Spread of the open loop (OL) ensemble (between 5th and 95th percentiles) and the 10 reference runs at (a, d, g, j) Powassan, (b, e, h, k) TVC , and (c, f, i, l) Rogers Pass for (a-c) the backscatter at 13.5 GHz, (d-f) the backscatter at 17.25 GHz, (g-i) for snow height , and (j-l) SWE for the winter 2022-2023.

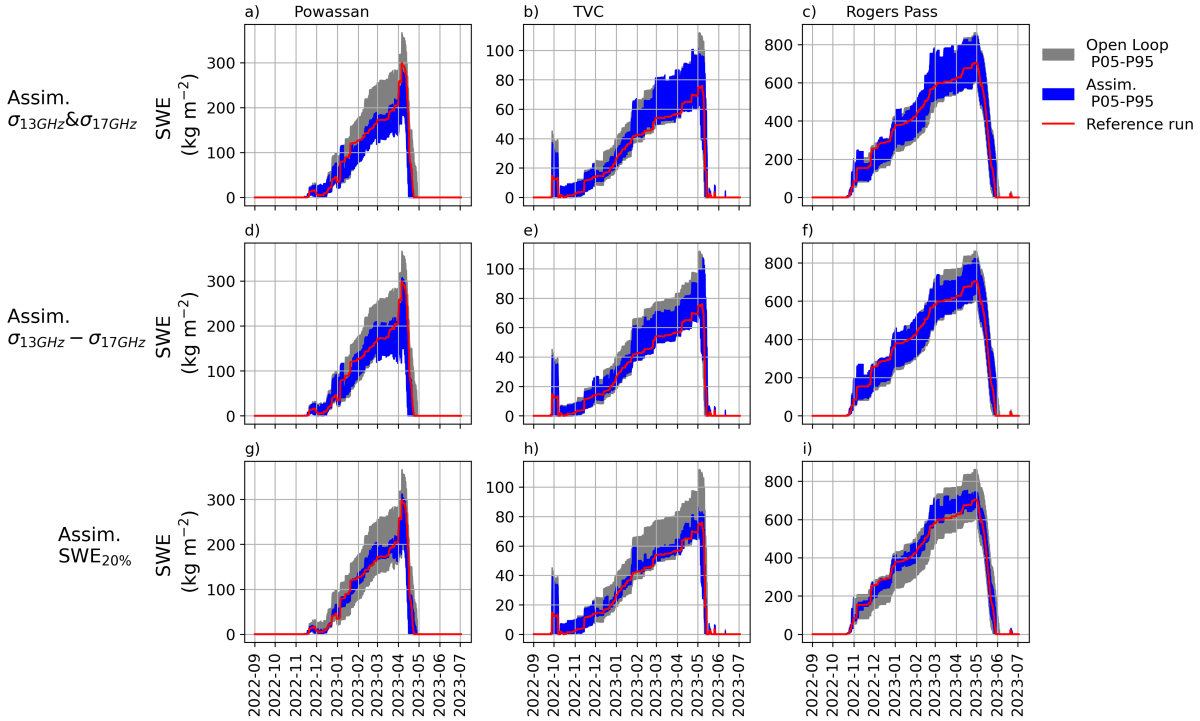

Figure S4. Results of the assimilation of the reference run #1 for the 2022-2023 snow season at (a,d,g) Powassan, (b,e,h) TVC, and (c,f,i) Rogers Pass. (a-c) are the results of assimilating both backscatter synthetic observations at 13.5 GHz and 17.25 GHz simultaneously, (d-f) for the assimilation of the difference if backscatter synthetic observations at 13.5 GHz and 17.25 GHz, and (g-i) for the assimilation of SWE synthetic observations with an error of 20 %. The gray envelope shows the spread between the 5th and 95th percentiles of the open loop (OL) without assimilation, while the blue envelope shows the results of the assimilation (5th to 95th percentiles) and the corresponding reference run is in red.

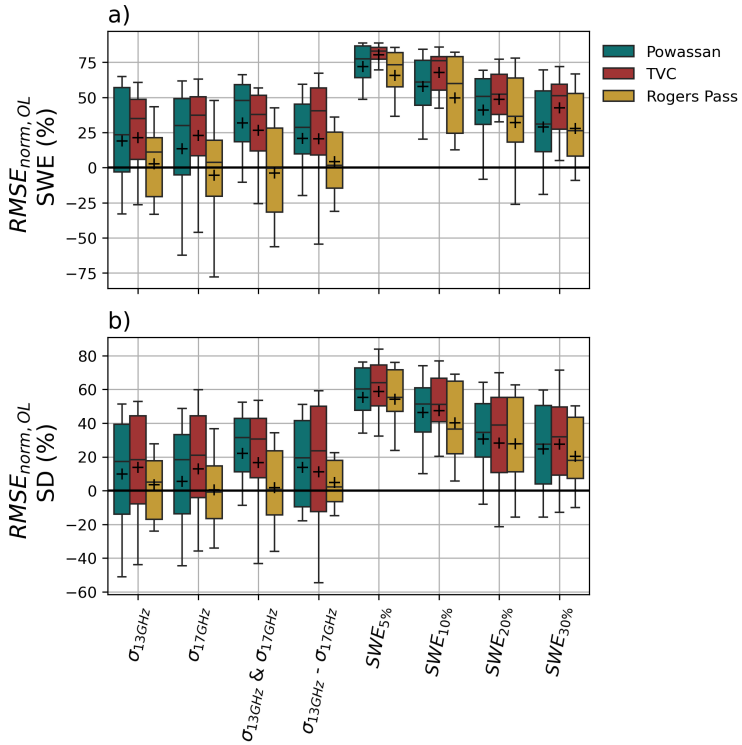

Figure S5. Normalized $RMSE$ against the open loop at all the observation times over all the different runs for the three winter seasons (a) for SWE prediction (b) and snow depth prediction at the three sites based on different inputs being assimilated. Box plots show median (center line), interquartile range (box), 10th–90th percentiles (whiskers), and mean (+). No outliers are shown for clarity.

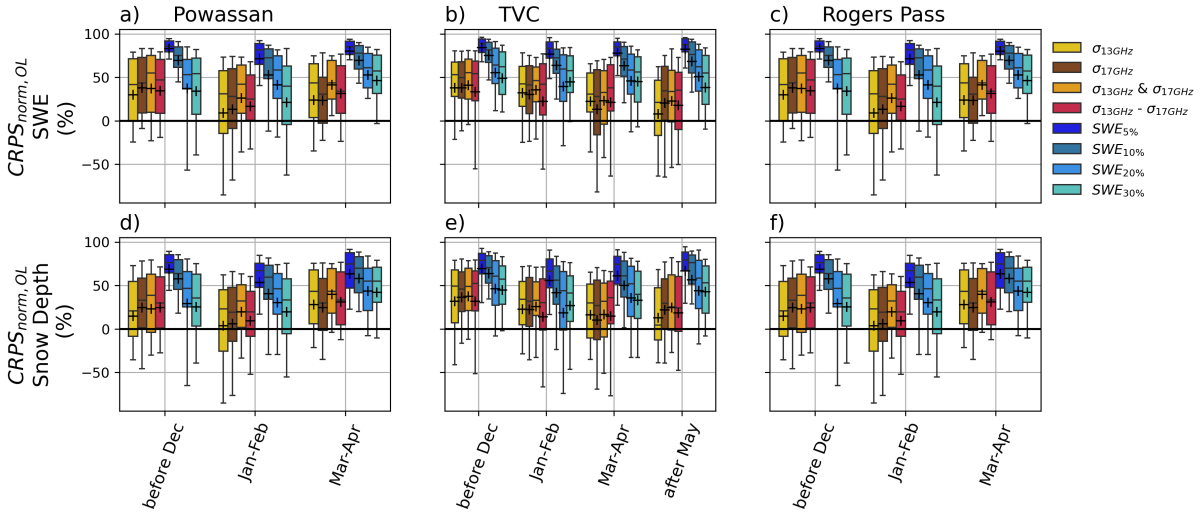

Figure S6. Normalized $CRPS$ against the open loop (OL) at observation times for all the different runs and the three winter seasons for (a-c) SWE prediction and (d-f) snow depth prediction for (a,d) Powassan, (b,e) TVC, and (c,f) Rogers Pass based on the month of the observations. Box plots show median (center line), interquartile range (box), 10th–90th percentiles (whiskers), and mean (+). No outliers are shown for clarity.

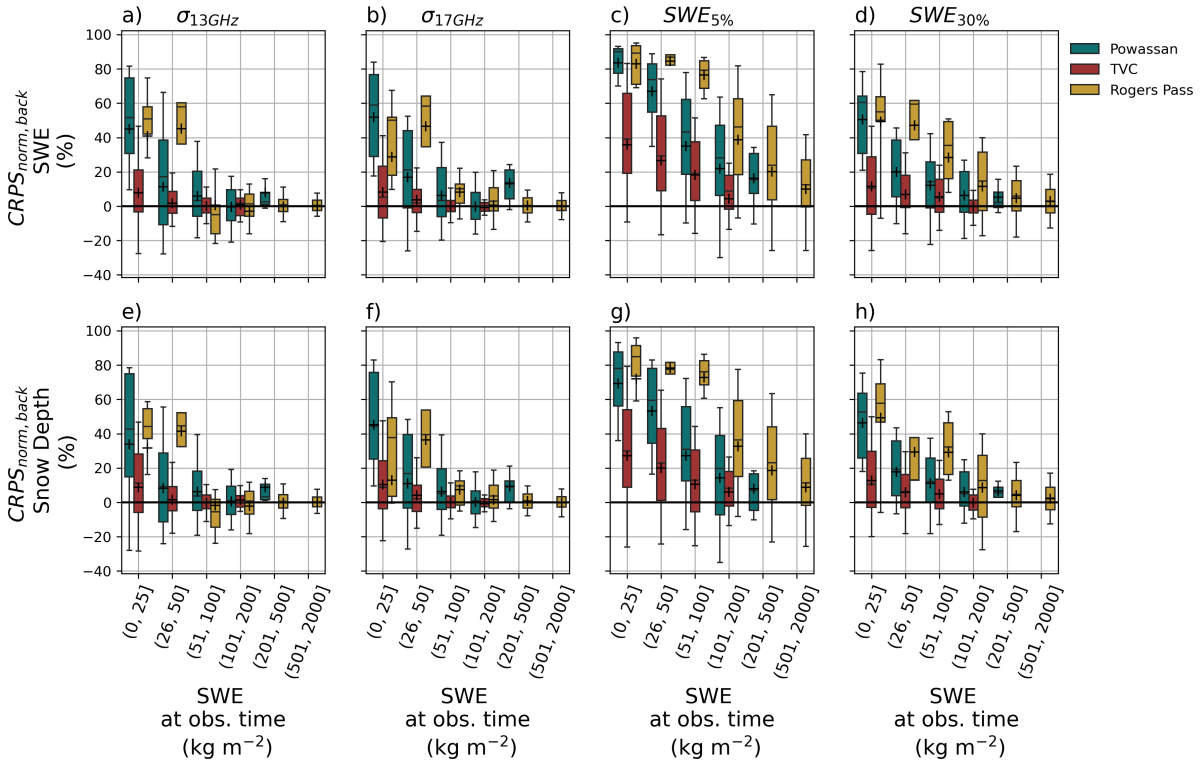

Figure S7. Normalized $CRPS$ against the background particles as a function of SWE values at the observation times aggregated over all the different runs and the three winter seasons for (a-d) SWE prediction and (e-h) snow depth prediction for the assimilation experiments with (a,e) backscatter observations at 13.25 GHz, (b,f) with backscatter observations at 17.5 GHz, (c,g) with SWE observations with an uncertainty of 5 % and (d,h) with SWE observations with an uncertainty of 30 %. The results are not shown for all the assimilation experiments for conciseness. As an example, the interval (26,50] signifies that 26 is excluded and 50 included in the interval. Box plots show median (center line), interquartile range (box), 10th–90th percentiles (whiskers), and mean (+). No outliers are shown for clarity..

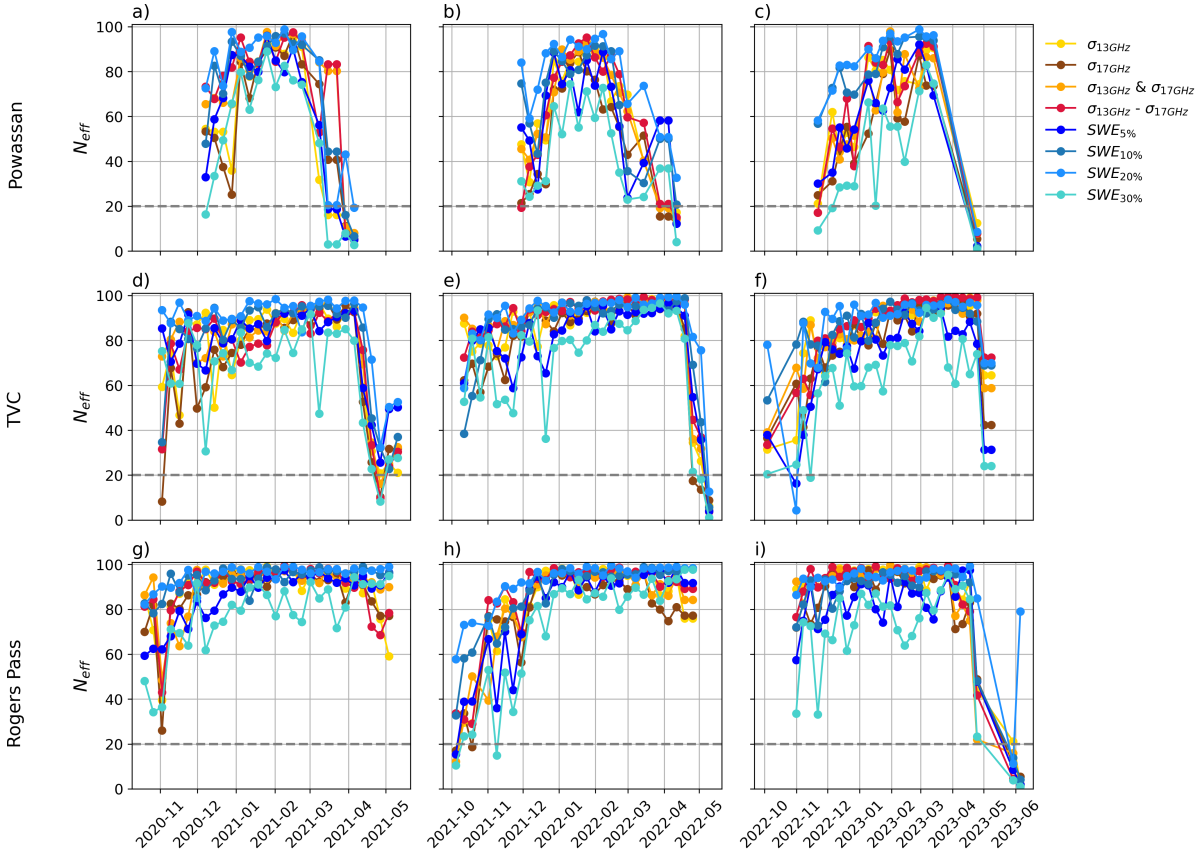

Figure S8. Evolution over time of the effective sample size (N_{eff}, Eq. 7 of the main manuscript) averaged over the 10 iterations for each winter season and for (a-c) Powassan, (d-f) TVC, and (g-i) Rogers Pass. The horizontal dashed line represents the 20 % threshold below which degeneracy is assumed to occur.